CONTROL OF SURFACE PLASMON EXCITATION VIA THE SCATTERING OF LIGHT BY A NANOPARTICLE

A. A. Zharov [a,b], **A. A. Zharov, Jr.** [a,b], **N. A. Zharova** [c*]

[a] *Institute for Physics of Microstructures, Russian Academy of Sciences*
603950, Nizhny Novgorod, Russia

[b] *Lobachevsky State University*
603950, Nizhny Novgorod, Russia

[c] *Institute of Applied Physics, Russian Academy of Sciences*
603950, Nizhny Novgorod, Russia

We study an excitation of surface plasmons (SPs) due to the scattering of light by a dipole nanoparticle located near a flat air–metal interface. It is well known that such a scattering can reveal asymmetric behavior of excited SPs with respect to the plane of incidence of light. This asymmetric SP excitation, which takes place at the incidence of elliptically polarized light, is often associated with the so-called photonic spin Hall effect caused by the interplay between rotating polarization of a nanoparticle and the intrinsic field angular momentum of the SP. We show that this photonic spin Hall effect can be applied for the SP excitation control, which allows managing the SP directivity pattern and amplitude. The possibilities of SP control can also be extended using nanoparticles with anisotropic polarizability. We believe that manipulations with SPs at a nanometer scale may find some applications in modern nanoplasmonics.

1. INTRODUCTION

Surface plasmon (SP) is a specific kind of electromagnetic excitations localized in the vicinity of the interface between a dielectric medium and a metal [1–4]. The electromagnetic field confinement near the metal–dielectric interface is provided by the free electron plasma of metals making the real part of the metal dielectric permittivity negative in a wide range of frequencies up to the near-ultraviolet domain. To date, SPs are one of the most relevant objects for intended use in light nanolocalization and light nanofocusing [5–9]. The SP control at a nanometer scale is recently attracting great interest due to a number of possible applications in different fields of contemporary nanophotonics, including medicine [10], biology and chemistry [5], nanolasing [11], and integrated optics [12, 13]. At the same time, the manipulations with SPs are somewhat complicated because of the absence of direct coupling between SPs and incident light. An SP is an electromagnetic excitation that is slowed down in comparison with the bulk wave, and only near-field excitation of an SP is possible. Thus, some additional optical elements generating higher spatial harmonics of the electromagnetic field are required to excite an SP. Actually, this can be done by any defect on the metal surface or by a nanoparticle located near the interface. It is known that the scattering of an elliptically polarized light wave by a nanoparticle or a nanowire may result in asymmetric excitation of an SP with respect to the plane of incidence [14]. This effect is often attributed to the so-called photonic spin Hall effect [15–18], which, in other words, is a manifestation of the interplay between rotating polarization of the nanoparticle and the SP intrinsic field angular momentum, which is sometimes associated with the SP spin [19–21]. Based on the concept of asymmetric SP excitation, the all-dielectric nanoantenna of special design is suggested [22]. It seems attractive to use the directional SP excitation for manipulations with SPs at a nanometer scale.

For this purpose, for example, we can explore scattering of an SP by subwavelength holes in metallic films [23, 24]. In elegant paper [25], it was shown that a

* E-mail: zhani@appl.sci-nnov.ru

point-like dipole with a definite (in the general case, elliptic) polarization placed near a metal–dielectric interface excites SPs with the directivity pattern strongly dependent on the dipole polarization. This means that SP radiation can be potentially controllable even by a point-like dipole.

In this paper, we study possibilities for control of SP excitation by means of incident light scattered by a nanoparticle located near the air–metal interface. Basing on an analytic solution and numerical analysis, we demonstrate that the dominant direction of SP propagation and the whole directivity pattern can be effectively managed by means of the angle of incidence, ellipticity of light, anisotropic nanoparticle orientation, and the nanoparticle position above the interface. We believe that directional excitation of SPs may broaden the field of possible plasmonic applications.

This paper is organized as follows. In Sec. 2, we give an analytic solution of the scattering problem. In Sec. 3, we present the obtained results and their discussion. In this section, we consider the SP excitation by a dipole nanoparticle with isotropic and anisotropic polarizabilities and demonstrate their potential to become a useful tool for manipulation of SPs. Finally, Sec. 4 concludes the paper.

2. THE SP EXCITATION DUE TO LIGHT SCATTERING BY A NANOPARTICLE. MATHEMATICAL FORMALISM

It is well known [2] that an SP guided by the interface between two nonmagnetic media has a TM polarization with two components of the electric field: along the wavevector **h** and normal to the interface with the phase shift $\pi/2$, due to the inhomogeneous type of the wave. Thus, the SP has a field angular momentum, which is often referred to as the SP spin oriented in the plane of the interface perpendicular to the wavevector **h**. We note that the field angular momentum is an inherent property of any inhomogeneous electromagnetic wave. Another important property of SPs is their nonradiating character because their phase velocity is smaller than the speed of light in the surrounding dielectric medium. This, in turn, means that according to the reciprocity principle, an SP cannot be directly excited by an incident bulk electromagnetic wave. This feature results in the necessity to use some optical couplers for SP excitation that generate higher spatial harmonics of the incident field, including nonpropagating near fields. There are well-known resonant prism couplers in Otto [26] and Kretchmann–Raether [27, 28] ge-
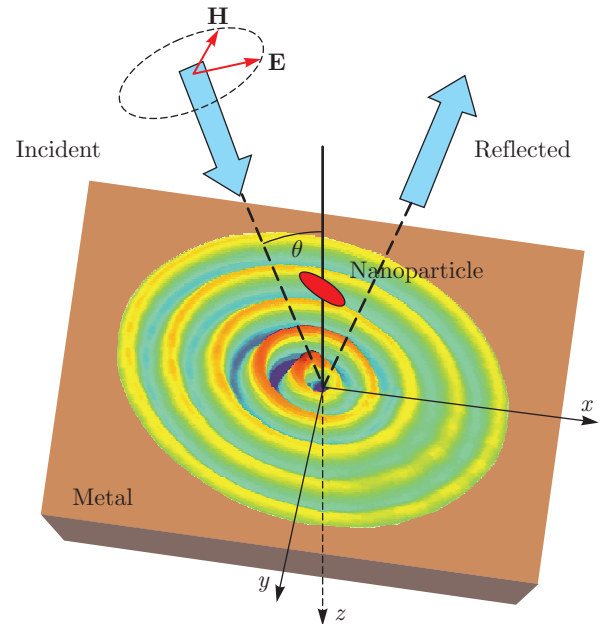

Fig. 1. Schematic geometry of the problem of SP excitation via the scattering of light by a dipole nanoparticle

ometries of attenuated total reflection (see also [29]), resonant grating coupling [30], so-called end-fire coupling of volume and surface waves [31] which occurs at the irradiation of the interface from the end side, or simply scattering of light by defects in the vicinity of the interface, which also leads to the emerging of near-field components. Below, we consider a simplified example of the scattering of elliptically polarized light by either a spherical or an elliptical dipole nanoparticle located near the air–metal interface to demonstrate quite wide possibilities of manipulations with excited SPs.

Let the air–metal interface be located at the plane $z = 0$ and the nanoparticle has coordinates $x = 0$, $y = 0$, $z = -a$, as is shown in Fig. 1. The incident elliptically polarized wave is a superposition of two plane TE and TM linear-polarized waves shifted in phase by some value Ψ. In the chosen coordinate system (see Fig. 1), the Cartesian components of those waves can be represented as

$$
\begin{aligned}
H_y &= A_0 \exp\left(-ik_z z - ik_x x\right), \\
E_x &= \frac{k_z}{k_0} A_0 \exp\left(-ik_z z - ik_x x\right), \\
E_z &= -\frac{k_x}{k_0} A_0 \exp\left(-ik_z z - ik_x x\right)
\end{aligned}
\tag{1}
$$

for the TM mode and

$$E_y = B_0 e^{i\Psi} \exp\left(-ik_z z - ik_x x\right),$$

$$H_x = \frac{k_z}{k_0} B_0 e^{i\Psi} \exp\left(-ik_z z - ik_x x\right), \qquad (2)$$

$$H_z = \frac{k_x}{k_0} B_0 e^{i\Psi} \exp\left(-ik_z z - ik_x x\right)$$

for the TE mode, where $k_0 = \omega/c$ is the wavenumber in free space, ω is the frequency of light (it is supposed that time-dependent electromagnetic field obeys the harmonic law, i.e., is proportional to $\exp\left(i\omega t\right)$), $k_z = k_0 \cos\theta$ and $k_x = k_0 \sin\theta$ are the wavevector components, θ is the angle of incidence, and the ratio A_0/B_0 and the phase Ψ (A_0 and B_0 are assumed to be real) define the eccentricity and orientation of the polarization ellipse of incident light. For example, $A_0 = B_0$ and $\Psi = \pi/2$ correspond to the circular polarization, while $A_0 \neq 0$, $B_0 = 0$ and $A_0 = 0$, $B_0 \neq 0$ to the respective pure TM and pure TE polarizations.

To solve the scattering problem, we start from the Maxwell equations with the dipole nanoparticle regarded as a point-like dipole,

$$\nabla \times \mathbf{E} = -ik_0 \mathbf{H},$$

$$\nabla \times \mathbf{H} = ik_0 \epsilon(z)\mathbf{E} + \frac{4\pi}{c}\mathbf{j}\delta(x)\delta(y)\delta(z+a), \qquad (3)$$

where $\mathbf{j} = i\omega\mathbf{p} = i\omega\hat{\alpha}\mathbf{E}$ is the electric current density flowing in the nanoparticle, $\mathbf{p}$ is the dipole moment, and $\hat{\alpha}$ is the tensor of polarizability of the nanoparticle. For a spherical homogeneous nanoparticle, $\hat{\alpha}$ is a scalar quantity,

$$\hat{\alpha} = \alpha = d^3 \frac{\epsilon_p - 1}{\epsilon_p + 2}, \qquad (4)$$

where ϵ_p is the dielectric permittivity of the nanoparticle material and d is the nanoparticle radius, which must be less than all electromagnetic characteristic scales such as the wavelength and skin-layer depth. Applying the spatial Fourier transformation along lateral coordinates x and y, we arrive at the set of equations

$$ih_y\mathcal{E}_z + \frac{d\mathcal{E}_y}{dz} = ik_0\mathcal{H}_x,$$

$$ih_x\mathcal{E}_z + \frac{d\mathcal{E}_x}{dz} = -ik_0\mathcal{H}_y,$$

$$h_x\mathcal{E}_y - h_y\mathcal{E}_x = k_0\mathcal{H}_z,$$

$$-ih_y\mathcal{H}_z - \frac{d\mathcal{H}_y}{dz} = ik_0\epsilon(z)\mathcal{E}_x + \frac{4\pi}{c}j_x\delta(z+a), \qquad (5)$$

$$ih_x\mathcal{H}_z + \frac{d\mathcal{H}_x}{dz} = ik_0\epsilon(z)\mathcal{E}_y + \frac{4\pi}{c}j_y\delta(z+a),$$

$$-h_x\mathcal{H}_y + h_y\mathcal{H}_x = k_0\epsilon(z)\mathcal{E}_z - i\frac{4\pi}{c}j_z\delta(z+a).$$

The effective surface currents j_x, j_y, and j_z in Eqs. (5) are determined by the superposition of incident, reflected, and SP electric fields. Currently, we keep the symbols $j_{x,y,z}$ and take their explicit dependences on $\mathbf{E}$ into account later, at the final stage of calculations. Tangential components of the electric, $\mathbf{E}_\tau$, and magnetic, $\mathbf{H}_\tau$, fields have to satisfy boundary conditions at the air–metal interface $z = 0$ and at the plane $z = -a$ of nanoparticle location. At $z = 0$, we should apply the continuity conditions for $\mathbf{E}_\tau$ and $\mathbf{H}_\tau$, but at $z = -a$ both $\mathbf{E}_\tau$ and $\mathbf{H}_\tau$ are discontinuous due to the effective polarization surface current. We note that j_z leads to a jump in $\mathbf{E}_\tau$, and therefore the normal surface electric current is equivalent to the tangential magnetic surface current. This result can be obtained by expressing E_z via $j_z\delta(z+a)$ in the second equation in (3) and substituting this expression in the first equation in (3) and subsequently integrating $dE_{x,y}/dz$ over z in the vicinity of $z = -a$. Maxwell equations (3) yield the boundary conditions

$$[\mathcal{H}_y]|_{z=-a} = -\frac{4\pi}{c}j_x, \quad [\mathcal{H}_x]|_{z=-a} = \frac{4\pi}{c}j_y,$$

$$[\mathcal{E}_y]|_{z=-a} = \frac{4\pi h_y}{\omega}j_z, \quad [\mathcal{E}_x]|_{z=-a} = \frac{4\pi h_x}{\omega}j_z, \qquad (6)$$

$$[\mathcal{H}_{x,y}]|_{z=0} = 0, \quad [\mathcal{E}_{x,y}]|_{z=0} = 0,$$

where square brackets denote the jumps of the corresponding quantities. In the regions free of electromagnetic sources, the electric field components can be expressed through the magnetic field components:

$$\mathcal{E}_x = -\frac{h_y}{k_0\epsilon(z)}\mathcal{H}_z - \frac{1}{ik_0\epsilon(z)}\frac{d\mathcal{H}_y}{dz},$$

$$\mathcal{E}_y = \frac{h_x}{k_0\epsilon(z)}\mathcal{H}_z + \frac{1}{ik_0\epsilon(z)}\frac{d\mathcal{H}_x}{dz}, \qquad (7)$$

$$\mathcal{E}_z = -\frac{h_x}{k_0\epsilon(z)}\mathcal{H}_y + \frac{h_y}{k_0\epsilon(z)}\mathcal{H}_x.$$

The magnetic field satisfies the Helmholtz equation

$$\frac{d^2\mathbf{H}}{dz^2} + (k_0^2\epsilon(z) - h^2)\mathbf{H} = 0, \qquad (8)$$

where $h^2 = h_x^2 + h_y^2$. It is convenient to rewrite relations (7) by means of Eqs. (5) for the tangential field components only. After that, we obtain

$$\mathcal{E}_x = -\frac{1}{ik_0\epsilon(z)\Delta}\left(1 - \frac{h_x^2}{k_0^2\epsilon(z)}\right)\frac{d\mathcal{H}_y}{dz} -$$

$$- \frac{h_x h_y}{ik_0^3\epsilon(z)^2\Delta}\frac{d\mathcal{H}_x}{dz},$$

$$\mathcal{E}_y = \frac{1}{ik_0\epsilon(z)\Delta}\left(1 - \frac{h_y^2}{k_0^2\epsilon(z)}\right)\frac{d\mathcal{H}_x}{dz} + \qquad (9)$$

$$+ \frac{h_x h_y}{ik_0^3\epsilon(z)^2\Delta}\frac{d\mathcal{H}_y}{dz},$$

$$\Delta = 1 - \frac{h^2}{k_0^2\epsilon(z)}.$$

Using the obvious solution of Eq. (8) in each region bounded by the planes $z = -a$ and $z = 0$ and taking zero values of the slow field with $h^2 > k_0^2 \epsilon(z)$ at $\pm\infty$ into account, we can obtain explicit expressions for tangential components of the electromagnetic field:

$$\mathcal{H}_x = A e^{\varkappa_0(z+a)}, \quad \mathcal{H}_y = B e^{\varkappa_0(z+a)},$$

$$\mathcal{E}_x = \left(-\frac{\varkappa_0(1 - h_x^2/k_0^2)}{i k_0 \Delta_0} B - \frac{\varkappa_0 h_x h_y}{i k_0^3 \Delta_0} A \right) \times$$
$$\times\, e^{\varkappa_0(z+a)}, \qquad (10)$$

$$\mathcal{E}_y = \left(\frac{\varkappa_0(1 - h_y^2/k_0^2)}{i k_0 \Delta_0} A - \frac{\varkappa_0 h_x h_y}{i k_0^3 \Delta_0} B \right) \times$$
$$\times\, e^{\varkappa_0(z+a)}$$

for $z < -a$,

$$\mathcal{H}_x = C_1 e^{\varkappa_0(z+a)} + D_1 e^{-\varkappa_0(z+a)},$$
$$\mathcal{H}_y = C_2 e^{\varkappa_0(z+a)} + D_2 e^{-\varkappa_0(z+a)},$$
$$\mathcal{E}_x = -\frac{\varkappa_0(1 - h_x^2/k_0^2)}{i k_0 \Delta_0} \times$$
$$\times \left(C_2 e^{\varkappa_0(z+a)} - D_2 e^{-\varkappa_0(z+a)} \right) -$$
$$- \frac{\varkappa_0 h_x h_y}{i k_0^3 \Delta_0} \left(C_1 e^{\varkappa_0(z+a)} - D_1 e^{-\varkappa_0(z+a)} \right), \quad (11)$$
$$\mathcal{E}_y = \frac{\varkappa_0(1 - h_y^2/k_0^2)}{i k_0 \Delta_0} \times$$
$$\times \left(C_1 e^{\varkappa_0(z+a)} - D_1 e^{-\varkappa_0(z+a)} \right) -$$
$$- \frac{\varkappa_0 h_x h_y}{i k_0^3 \Delta_0} \left(C_2 e^{\varkappa_0(z+a)} - D_2 e^{-\varkappa_0(z+a)} \right)$$

for $-a < z < 0$, and

$$\mathcal{H}_x = F e^{-\varkappa_m(z+a)}, \quad \mathcal{H}_y = G e^{-\varkappa_m(z+a)},$$

$$\mathcal{E}_x = \left(\frac{\varkappa_m}{i k_0 \epsilon_m \Delta_m} \left(1 - \frac{h_x^2}{k_0^2 \epsilon_m} \right) G + \right.$$
$$\left. + \frac{\varkappa_m h_x h_y}{i k_0^3 \epsilon_m^2 \Delta_m} F \right) e^{-\varkappa_m(z+a)},$$
$$\qquad (12)$$
$$\mathcal{E}_y = -\left(\frac{\varkappa_m}{i k_0 \epsilon_m \Delta_m} \left(1 - \frac{h_y^2}{k_0^2 \epsilon_m} \right) F - \right.$$
$$\left. - \frac{\varkappa_m h_x h_y}{i k_0^3 \epsilon_m^2 \Delta_m} G \right) e^{-\varkappa_m(z+a)}$$

for $z > 0$. Here,

$$\varkappa_0 = \sqrt{h^2 - k_0^2}, \quad \varkappa_m = \sqrt{h^2 - k_0^2 \epsilon_m},$$

$$\Delta_0 = 1 - \frac{h^2}{k_0^2}, \quad \Delta_m = 1 - \frac{h^2}{k_0^2 \epsilon_m},$$

ϵ_m is the dielectric permittivity of metal, and the constants A, B, $C_{1,2}$, $D_{1,2}$, F, and G should be found from the field matching at $z = -a$ and $z = 0$ according to boundary conditions (6). The calculation of these constants is a straightforward but quite cumbersome procedure, which we omit and quote only the final result:

$$G = \frac{\Delta_G}{\Sigma}, \quad F = \frac{\Delta_F}{\Sigma},$$

$$\Delta_G = \frac{2 h_x h_y}{\varkappa_0 \varkappa_m} \left(1 - \frac{1}{\epsilon_m} \right) \tilde{D}_1 + \frac{2 k_0^2}{\varkappa_0^2} \times$$
$$\times \left[\Delta_0 + \frac{\varkappa_0}{\varkappa_m} \left(1 - \frac{h_y^2}{k_0^2 \epsilon_m} \right) - \right.$$
$$\left. - \frac{h_x^2}{k_0^2} \left(1 + \frac{\varkappa_0}{\varkappa_m} \right) \right] \tilde{D}_2,$$

$$\Delta_F = \frac{2 k_0^2}{\varkappa_0^2} \left[\Delta_0 + \frac{\varkappa_0}{\varkappa_m} \left(1 - \frac{h_x^2}{k_0^2 \epsilon_m} \right) - \right.$$
$$\left. - \frac{h_y^2}{k_0^2} \left(1 + \frac{\varkappa_0}{\varkappa_m} \right) \right] \tilde{D}_1 + \qquad (13)$$
$$+ \frac{2 h_x h_y}{\varkappa_0 \varkappa_m} \left(1 - \frac{1}{\epsilon_m} \right) \tilde{D}_2,$$

$$\tilde{D}_{1,2} = D_{1,2} e^{-\varkappa_0 a},$$

$$D_1 = -\frac{2\pi}{c} \left(i \frac{h_y}{\varkappa_0} j_z - j_y \right),$$

$$D_2 = \frac{2\pi}{c} \left(i \frac{h_x}{\varkappa_0} j_z - j_x \right),$$

$$C_1 = F e^{-\varkappa_0 a} - D_1 e^{-2\varkappa_0 a},$$

$$C_2 = G e^{-\varkappa_0 a} - D_2 e^{-2\varkappa_0 a},$$

$$A = C_1 + D_1 - \frac{4\pi}{c} j_y, \quad B = C_2 + D_2 - \frac{4\pi}{c} j_x,$$

where $\Sigma = -(\varkappa_m/\epsilon_m + \varkappa_0)(1/\varkappa_m + 1/\varkappa_0)$. We note that the expressions for all the constants G, F, $C_{1,2}$, A, and B include the factor $1/\Sigma$, and the equation

$$\frac{\varkappa_m}{\epsilon_m} + \varkappa_0 = 0 \qquad (14)$$

is the dispersion relation for SPs guided by an air–metal interface. At the same time, the roots of Eq. (14) are the poles of the integrand in the inverse Fourier transform. Therefore, it becomes possible to analytically calculate the SP amplitude based on contour integration in the complex plane (h_x, h_y). The solution of Eq. (14) for h leads to the well-known result (see, e. g., [2])

$$h^2 = k_0^2 \frac{\epsilon_m}{\epsilon_m + 1}, \qquad (15)$$

where the real part of the metal permittivity must be negative. The imaginary part of ϵ_m gives the rule for choosing the integration contour in the vicinity of the singularities. Thus, in order to determine the wave field

in coordinate space, we should apply the inverse Fourier transformation to all expressions (10)–(12), which allows finding the electromagnetic field structure in the whole space. For the amplitudes of the tangential magnetic field, we have

$$
H_{x,y}(x,y,z) = \iint \mathcal{H}_{x,y}(z, h_x, h_y) \times
$$
$$
\times \exp(-i h_x x - i h_y y) \frac{dh_x dh_y}{(2\pi)^2}, \quad (16)
$$

where $\mathcal{H}$ stands for Fourier components given by formulas (10)–(12) with the constants determined in Eqs. (13). It is more convenient to do the integration in terms of polar coordinates h and ϕ:

$$
h_x = h \cos\phi, \quad h_y = h \sin\phi, \quad dh_x dh_y = h\, dh\, d\phi. \quad (17)
$$

To perform the contour integration, we should multiply both numerator and denominator of any integrand in Eq. (16) by the value $\varkappa_m / \epsilon_m - \varkappa_0$, which enables extracting simple poles. The corresponding residues of the integrand after the integration over h define the angle dependence of the SP far-field intensity (i. e., the directivity pattern). We show in what follows that the obtained approximate analytic results for the SP directivity patterns demonstrate good agreement with a full-wave numerical solution.

3. RESULTS AND DISCUSSION

After integration, we obtain the desired final expressions for $F(\phi, \omega, \theta)$ and $G(\phi, \omega, \theta)$, which define the SP directivity pattern written in terms of the one-fold inverse Fourier transform over the SP wavenumber of the tangential magnetic field components H_x and H_y at the interface $z = 0$:

$$
\begin{aligned}
F = {}& 2i k_0^2 \frac{\epsilon_m^2 (1 - \epsilon_m)}{\epsilon_m^2 - 1} \times \\
& \times \left(\sin^2\phi\, D_1 - \sin\phi \cos\phi\, D_2 \right) \times \\
& \times \exp\left(-\frac{k_0 a}{\sqrt{-(1 + \epsilon_m)}} \right), \\
G = {}& -2i k_0^2 \frac{\epsilon_m^2 (1 - \epsilon_m)}{\epsilon_m^2 - 1} \times \\
& \times \left(\sin\phi \cos\phi\, D_1 - \cos^2\phi\, D_2 \right) \times \\
& \times \exp\left(-\frac{k_0 a}{\sqrt{-(1 + \epsilon_m)}} \right), \\
D_1 = {}& -\frac{2\pi}{c} \left(i\sqrt{-\epsilon_m}\, \sin\phi\, j_z - j_y \right), \\
D_2 = {}& \frac{2\pi}{c} \left(i\sqrt{-\epsilon_m}\, \cos\phi\, j_z - j_x \right).
\end{aligned} \quad (18)
$$

For example, if j_z is shifted in phase by $\pi/2$ relative to j_x or j_y (which corresponds to elliptic polarization of the dipole moment), then D_1 or D_2 may become zero, which in turn results in an obvious asymmetry in the SP excitation, while if $j_z = 0$ and $j_x = j_y$, the SP excitation is symmetric. Below, we demonstrate the possibility of SP excitation control for several realistic examples. First of all, we recall that the electric current in Eqs. (18) is to be given as an extraneous current [32]. On the other hand, this current is induced by external incident and reflected electromagnetic waves along with the SP field. Including the electromagnetic field of the SP into consideration inevitably leads to an integral equation for the SP amplitude. The electromagnetic field of the excited SP changes the nanoparticle polarization induced by external (incident and reflected) light, and, strictly speaking, it is necessary to find nanoparticle polarization self-consistently. But the contribution of the SP field to the nanoparticle polarization is relatively small (proportional to $(k_0 d)^3 \exp(-2\kappa_0 a) \ll 1$ because the polarization current is proportional to the nanoparticle volume, i. e., is proportional to d^3), which gives us a reason to neglect the SP impact on the nanoparticle polarization. Thus, in order to calculate the values of electric currents in formulas (18), we should determine the electric field strength at the point of nanoparticle location $(x, y = 0, z = -a)$. This field is the sum of the fields of incident and reflected light:

$$
\begin{aligned}
E_x = {}& \cos\theta\, A_0 \left(e^{-i k_0 a \cos\theta} - \right. \\
& \left. - \frac{\epsilon_m \cos\theta + i\sqrt{\sin^2\theta - \epsilon_m}}{\epsilon_m \cos\theta - i\sqrt{\sin^2\theta - \epsilon_m}} e^{i k_0 a \cos\theta} \right), \\
E_y = {}& B_0 e^{i\Psi} \left(e^{-i k_0 a \cos\theta} + \right. \\
& \left. + \frac{\cos\theta + i\sqrt{\sin^2\theta - \epsilon_m}}{\cos\theta - i\sqrt{\sin^2\theta - \epsilon_m}} e^{i k_0 a \cos\theta} \right), \\
E_z = {}& -\sin\theta\, A_0 \left(e^{-i k_0 a \cos\theta} + \right. \\
& \left. + \frac{\epsilon_m \cos\theta + i\sqrt{\sin^2\theta - \epsilon_m}}{\epsilon_m \cos\theta - i\sqrt{\sin^2\theta - \epsilon_m}} e^{i k_0 a \cos\theta} \right).
\end{aligned} \quad (19)
$$

We recall that θ is the angle of incidence, A_0 and B_0 are the respective amplitudes of partial TM-polarized and TE-polarized waves, and Ψ is the phase shift between the TM and TE waves.
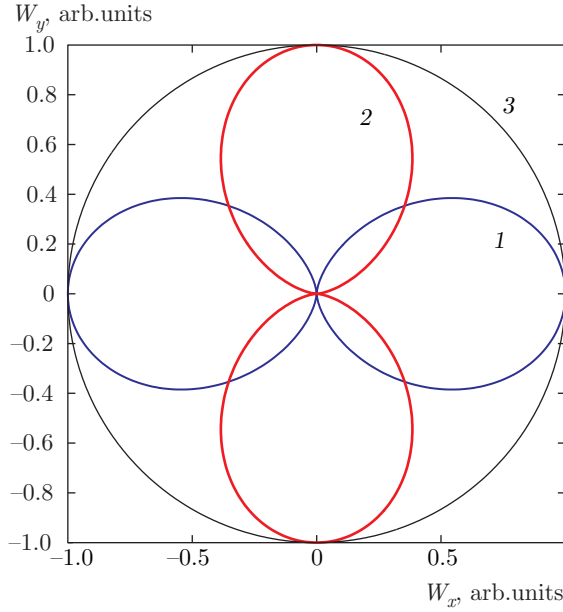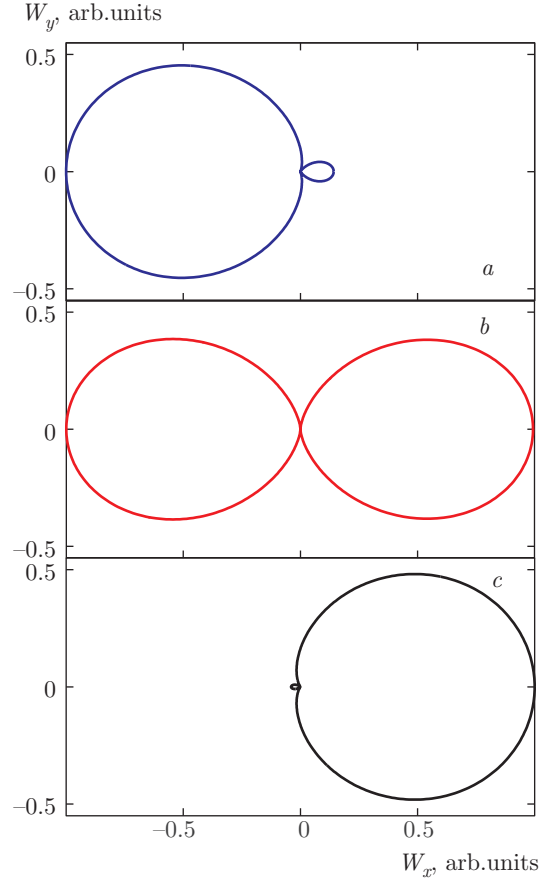
Fig. 2. Directivity patterns of the SP, $W(\phi) = |F|^2 + |G|^2$, in the case of TEM-polarized normally incident light ($\theta = 0$): curve *1* is a dipole-like pattern excited by a linearly polarized wave ($B_0 = 0$) with only the E_x component; curve *2* is a similar, but ortogonal pattern excited by a linearly polarized wave ($A_0 = 0$) with only the E_y component; curve *3* is a symmetric circular pattern excited by a circularly polarized wave with $E_y = iE_x$ ($B_0 = A_0$, $\Psi = \pi/2$); the radiation wavelength is $\lambda_0 = 500$ nm; the metal (silver) permittivity is $\varepsilon_m = -7.8191 - 0.7797i$

3.1. Excitation by a spherical nanoparticle

Variation of the angle of incidence and/or the nanoparticle position leads to a change in the phase and the amplitude of the full electromagnetic field of light (incident plus reflected), which results in a modification of the nanoparticle polarization ellipse up to inversion of the rotation direction of the dipole moment vector. In turn, it changes the conditions for SP excitation. Hence, we can expect different SP excitation modes including the possibility of scanning of the SP propagation direction. This fact is demonstrated in Figs. 2–4, where the directivity patterns $W(\phi) = |F|^2 + |G|^2$ (in arbitrary units) of excited SPs calculated in accordance with Eqs. (19) are shown. In Fig. 2, the directivity patterns of an SP excited by normally incident light are depicted for three cases of different polarizations. Curves *1* and *2* respectively display the SP excitation by light that is linearly polarized along the x and y axes. The SP directivity patterns have the form typical for dipole radiation, but nevertheless they significantly differ from a vacuum-radiating dipole. Indeed,

Fig. 3. Directivity patterns of the SP, $W(\phi) = |F|^2 + |G|^2$, in the case of oblique incidence of a linearly polarized TM wave ($\theta = \pi/8$) for three different positions of the particle: (*a*) $k_0 a \cos\theta = 0.5\pi$; (*b*) $k_0 a \cos\theta = 0.618\pi$; and (*c*) $k_0 a \cos\theta = 0.7857\pi$. The other parameters are the same as in Fig. 2
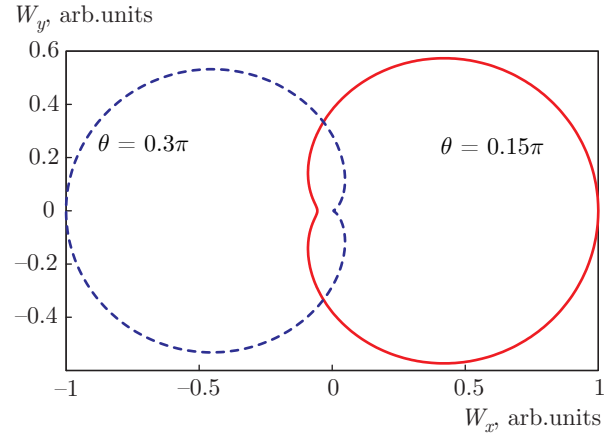
the vacuum dipole produces maximum radiation in the direction perpendicular to the dipole moment, but the maximum excitation of SP falls on the corresponding parallel direction. Such a difference is caused by polarization of radiated waves: dipole radiation in vacuum is transversely (TEM) polarized, whereas the excited surface plasmon mode is TM-polarized, and therefore has the electric field component along the wavevector. The symmetric circular directivity pattern of the SP emerges in the case of circular-polarized incident light (Fig. 2, curve *3*). The next figure (Fig. 3) shows the directivity patterns of the SP in the case of linearly TM-polarized light at oblique incidence and different positions of the nanoparticle above the interface. Figures 3*a,c* demonstrate an almost unidirectional excitation of the SP ("plasmonic projectors") in opposite directions depending on the location of the nanoparti-
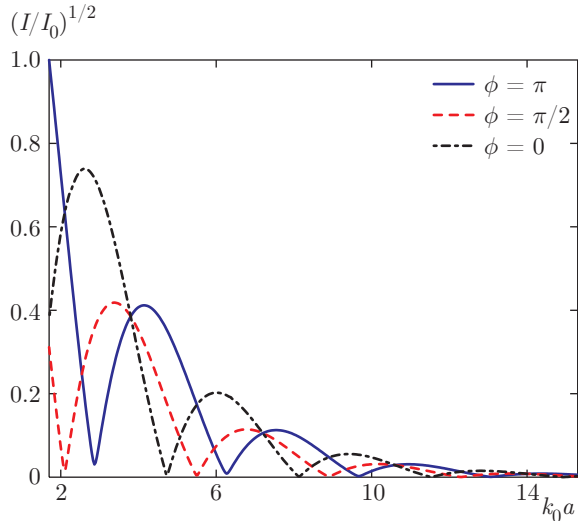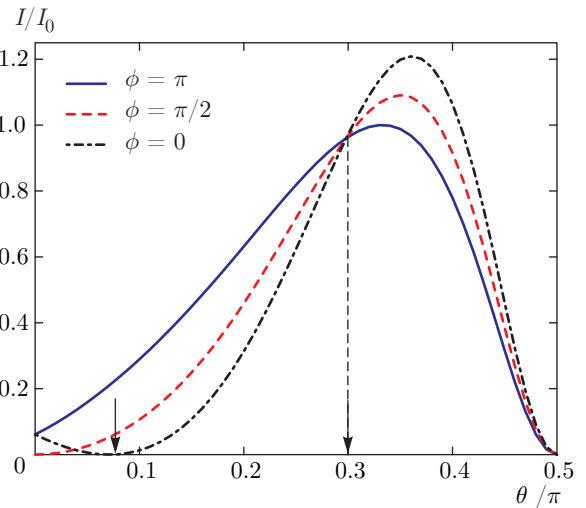
Fig. 4. Dependence of the (normalized) intensity of SP excitation on the nanoparticle position in the case of oblique incidence of a linearly polarized TM wave for forward ($\phi = 0$), backward ($\phi = \pi$), and sideward ($\phi = \pi/2$) directions of radiation; $\theta = \pi/8$, $B_0 = 0$, and the other parameters are the same as in Fig. 2
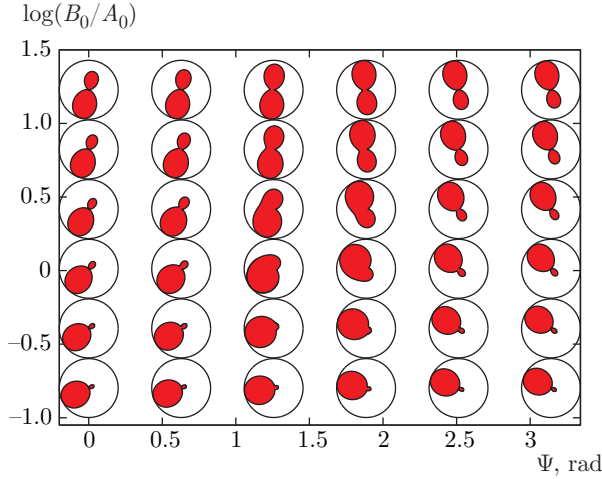

Fig. 5. Directivity patterns of the SP, $W(\phi) = |F|^2 + |G|^2$, in the case of oblique incidence of a linearly polarized TM wave ($B_0 = 0$, $k_0 a = \pi$) for two different angles of incidence: $\theta = 0.15\pi$ and $\theta = 0.3\pi$. The other parameters are the same as in Fig. 2

Fig. 6. The (normalized) intensity of SP excitation as a function of the angle of incidence in the case of a linearly polarized TM wave for forward ($\phi = 0$), backward ($\phi = \pi$), and sideward ($\phi = \pi/2$) directions of radiation; $B_0 = 0$, $k_0 a = 0.3\pi$, and the other parameters are the same as in Fig. 2. Arrows indicate specific incidence angles at which there is no forward radiation or the directivity pattern is symmetric

cle. It occurs due to the transverse angular momentum of the wave that resides in all kinds of inhomogeneous electromagnetic waves, including two interfering (incident and reflected) plane waves (as in the case considered here and also in [21]). The direction of the transverse angular momentum changes periodically along the z axis with the period $\Delta z = \pi/k_0 \cos\theta$, and this leads to a change in the direction of the nanoparticle dipole moment rotation. Because the SP also has the transverse angular momentum with a specific direction relative to the SP wavevector, the direction of SP excitation is determined so as to match the external field angular momentum of incident and reflected waves with that of the SP.

The intermediate situation (Fig. 3b) is characterized by symmetric SP excitation when the nanoparticle is located at the point where right-handed and left-handed rotation of the electromagnetic field in interfering incident and reflected waves supersede one another. Considerable changes in the directivity pattern from a highly anisotropic (as in Fig. 3a,c) to the symmetric one in the x direction (as in Fig. 3b) and a circularly symmetric one (at $k_0 a \cos\theta \approx 1.119\pi$, not shown) demonstrate the potential of its easy control. Figure 4 shows the intensity of the excited SP in three directions: forward (relative to the direction of the incident plane wave, i.e., the $+x$ direction), $\phi = 0$; backward, $\phi = \pi$, and sideward, $\phi = \pi/2$, as a function of the nanoparticle position ($z = -a$). The decrease in the

SP intensity when the nanoparticle moves away from the interface relates to the reduction of the scattered near-field from the nanoparticle. Along with the distance between the nanoparticle and the interface, the angle of incidence of light also affects the SP excitation because of the change in the phase shift between the incident and reflected waves at a fixed position of the nanoparticle. This is illustrated in Figs. 5 and 6.

Fig. 7. Directivity patterns of the SP excited by elliptically polarized ligth, which is a sum of TM and TE plane waves with different ratios of partial amplitudes, $B_0/A_0 = 0.2(1.5^2, 1.5^3, 1.5^4, 1.5^5, 1.5^6, 1.5^7)$, and different phase shifts $\Psi = (0, 0.2, 0.4, 0.6, 0.8, 1)\pi$; $k_0 a = 0.5\pi$, $\theta = 0.1\pi$, and the other parameters are the same as in Fig. 2

In Fig. 5, the directivity patterns of the SP excited by TM-polarized light at different angles of incidence are shown. We can see that changing the incidence angle induces strong changes in $W(\phi)$, and the direction of the SP propagation may even be inverted. In Fig. 6, the intensities of the excited SP in the forward ($\phi = 0$), backward ($\phi = \pi$), and sideward ($\phi = \pi/2$) directions are given as functions of the incidence angle. The characteristic angles of incidence corresponding to the case of vanishing forward radiation ($\theta \approx 0.07\pi$) and a symmetric directivity pattern ($\theta \approx 0.3\pi$) are shown in Fig. 6 by arrows. Thus, we can see that linearly polarized light already offers quite wide capabilities to adjust the SP directivity pattern, and this results from the transverse field angular momentum, which changes along the z axis and also depends on the angle of incidence θ.

Using the elliptically polarized incident electromagnetic waves, we can scan and switch the SP directivity pattern by both changing the phase shift Ψ (between the partial linear-polarized TE and TM incident waves) and varying the ratio of their amplitudes. Figure 7 demonstrates the potential of the considered system for easily scanning the directivity of an excited SP. Here, in the plane of parameters $(\Psi, \log B_0/A_0)$, the corresponding directivity patterns are depicted for the particular values $\Psi = (0, 0.2, 0.4, 0.6, 0.8, 1) \times \pi$ and $B_0/A_0 = 0.2(1.5^2, 1.5^3, 1.5^4, 1.5^5, 1.5^6, 1.5^7)$.

Figure 7 reveals that the most effective control of an SP can be realized by simply varying the amplitudes A_0 and B_0 (e. g., using an optical filter or a splitter), and the phase shift Ψ (e. g., using a delay line) at a fixed angle of incidence. Furthermore, it is necessary to note that a circularly polarized incident wave does not provide better conditions for an asymmetric unidirectional excitation of the SP. By contrast, the optimal excitation regime can be realized using an elliptically polarized incident wave with a particular orientation of the polarization ellipse due to a better matching of the nanoparticle polarization with the polarization of the excited SP.

3.2. Excitation by an anisotropic nanoparticle

The above calculations clearly exhibit different ways for manipulation of the SPs. Light scattered by nanoparticles can produce SPs propagating mainly unidirectionally as well as evenly in all directions, and the capability of scanning the directivity pattern may turn out to be useful in nanoplasmonic applications. All of those SP excitation modes strongly depend on light polarization, the angle of incidence, and the nanoparticle location above the interface. However, the scattering of light by a single nanoparticle actually never leads to the formation of a narrow SP directivity pattern. Nevertheless, we may expect a perfect unidirectional SP excitation due to the scattering of light by a lattice of dipole nanoparticles. The SP control can be broadened by means of an anisotropic scatterer, for example, an irregular-shaped nanoparticle described by the polarizability tensor $\hat{\alpha}$, and the orientation of the particle (and also of $\hat{\alpha}$) can be managed by the external constant electric field.

As a simple example, we let the nanoparticle shape be an ellipsoid of revolution and the nanoparticle itself be placed just on the interface such that the major axis of the ellipsoid is parallel to the interface and tilted with respect to the x axis at an angle β. In this case, the polarizability tensor has the form

$$\hat{\alpha} = \begin{pmatrix} \alpha_{xx} & \alpha_{xy} & 0 \\ \alpha_{yx} & \alpha_{yy} & 0 \\ 0 & 0 & \alpha_{zz} \end{pmatrix}, \quad (20)$$

where $\alpha_{xx} = \alpha^{(\perp)} + (\alpha^{(\parallel)} - \alpha^{(\perp)})\cos^2\beta$, $\alpha_{yy} = \alpha^{(\perp)} + (\alpha^{(\parallel)} - \alpha^{(\perp)})\sin^2\beta$, $\alpha_{zz} = \alpha^{(\perp)}$, $\alpha_{xy} = \alpha_{yx} = (\alpha^{(\parallel)} - \alpha^{(\perp)})\sin\beta\cos\beta$. Here, $\alpha^{(\parallel)}$ and $\alpha^{(\perp)}$ are

longitudinal and transverse parts of the ellipsoid polarizability tensor in principal axes given by [33]

$$\alpha^{(\perp)} = \frac{d_\perp^2 d_\parallel}{3} \frac{\epsilon_p - 1}{1 + 1/2(\epsilon_p - 1)(1 - n)},$$

$$\alpha^{(\parallel)} = \frac{d_\perp^2 d_\parallel}{3} \frac{\epsilon_p - 1}{1 + (\epsilon_p - 1)n},$$
(21)

where ϵ_p is the matter permittivity of the particle, $d_\perp$ and $d_\parallel$ are the principal semi-axes of the ellipsoid, and

$$n = \frac{1}{2} \left(\frac{d_\perp}{d_\parallel} \right)^2 \int_0^\infty \frac{d\xi}{(1 + \xi)^{3/2}(\xi + (d_\perp/d_\parallel)^2)}$$
(22)

is the so-called depolarization factor, which varies in the range $0 < n < 1$ with $n = 1/3$ corresponding to a sphere; $0 < n < 1/3$ relate to elongated and $1/3 < n < 1$ to oblate nanoparticles.

Let the nanoparticle be illuminated by obliquely incident TM linearly polarized light. According to Eqs. (19), the electric field of the incident wave at the nanoparticle location ($x = 0$, $y = 0$, $z = 0$) has the components

$$E_x = \frac{-2i \cos\theta \sqrt{\sin^2\theta - \epsilon_m}}{\epsilon_m \cos\theta - i\sqrt{\sin^2\theta - \epsilon_m}} A_0,$$

$$E_z = \frac{-2\epsilon_m \sin\theta \cos\theta}{\epsilon_m \cos\theta - i\sqrt{\sin^2\theta - \epsilon_m}} A_0.$$
(23)

Hence, the nanoparticle polarization can be written in the form

$$p_x = \alpha_{xx} E_x, \quad p_y = \alpha_{yx} E_x, \quad p_z = \alpha_{zz} E_z, \quad (24)$$

and it completely differs from light polarization, $\mathbf{p} \nparallel \mathbf{E}$. Moreover, absorption of light in the particle, which is described by a nonzero imaginary part of the polarizability tensor, can also change the nanopartile polarization ellipse and lead to an asymmetric excitation of the SP. The polarizability tensor components depend on the angle of nanoparticle rotation β relative to the projection of the wave electric field on the plane of the interface. Therefore, changing β results in changing the conditions for SP excitation. In Fig. 8, the SP directivity patterns at different β are shown. As mentioned above, the particle orientation can be controlled by an external constant electric field, which gives us a convenient tool for SP manipulation.

It is of interest to transform the field spectrum $E_z(h_x, h_y, z)$ at the interface $z = 0$ into real space (x, y), i.e., to find the spatial field structure
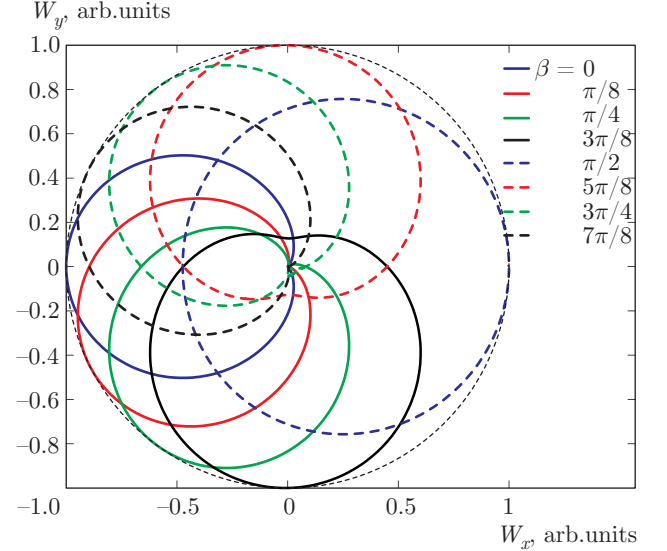
Fig. 8. Directivity patterns of the SP excited by TM polarized light incident on an elongated elliptical silver nanoparticle placed very close to the metal–air interface; calculations are performed for different angles β of the particle orientation. The ratio of the ellipsoid semi-axes is $d_\perp/d_\parallel = 0.2$, $n = 0.056$, $\epsilon_p = \epsilon_m = -7.8191 - 0.7797i$, $\theta = \pi/4$, and the other parameters are the same as in Fig. 2

$E_z(x, y, z = 0)$ of the excited SP. The results of such a Fourier transformation are depicted in Fig. 9a,c. We can clearly see an asymmetric excitation in agreement with the directivity patterns shown in Fig. 9b,d. We note that these directivity patterns (yellow (gray) areas) represent a more accurate numerical solution, where the radial component of the Poynting vector (calculated using the field distributions in Fig. 9a,c) was found as a function of the azimuthal angle. However, this directivity pattern nearly coincides with that of simplified analytic calculations described above (the black curve at the boundary of the yellow (gray) area). The similarity is a result of a very strong impact of the excited eigenmodes (of the singularities in integration, Eq. (16)).

Another type of polarization anisotropy originates in magnetized gyrotropic ferromagnetic particles, and here we can expect similar "photonic spin-dependent" effects of SP excitation to occur [34]. However, in the optical domain, the gyrotropy correction to the ferromagnetic nanoparticle polarizability tensor is very small (the nondiagonal component of the polarizability tensor is of the order of 10^{-3}), and the corresponding desired effect should be negligibly small as well.
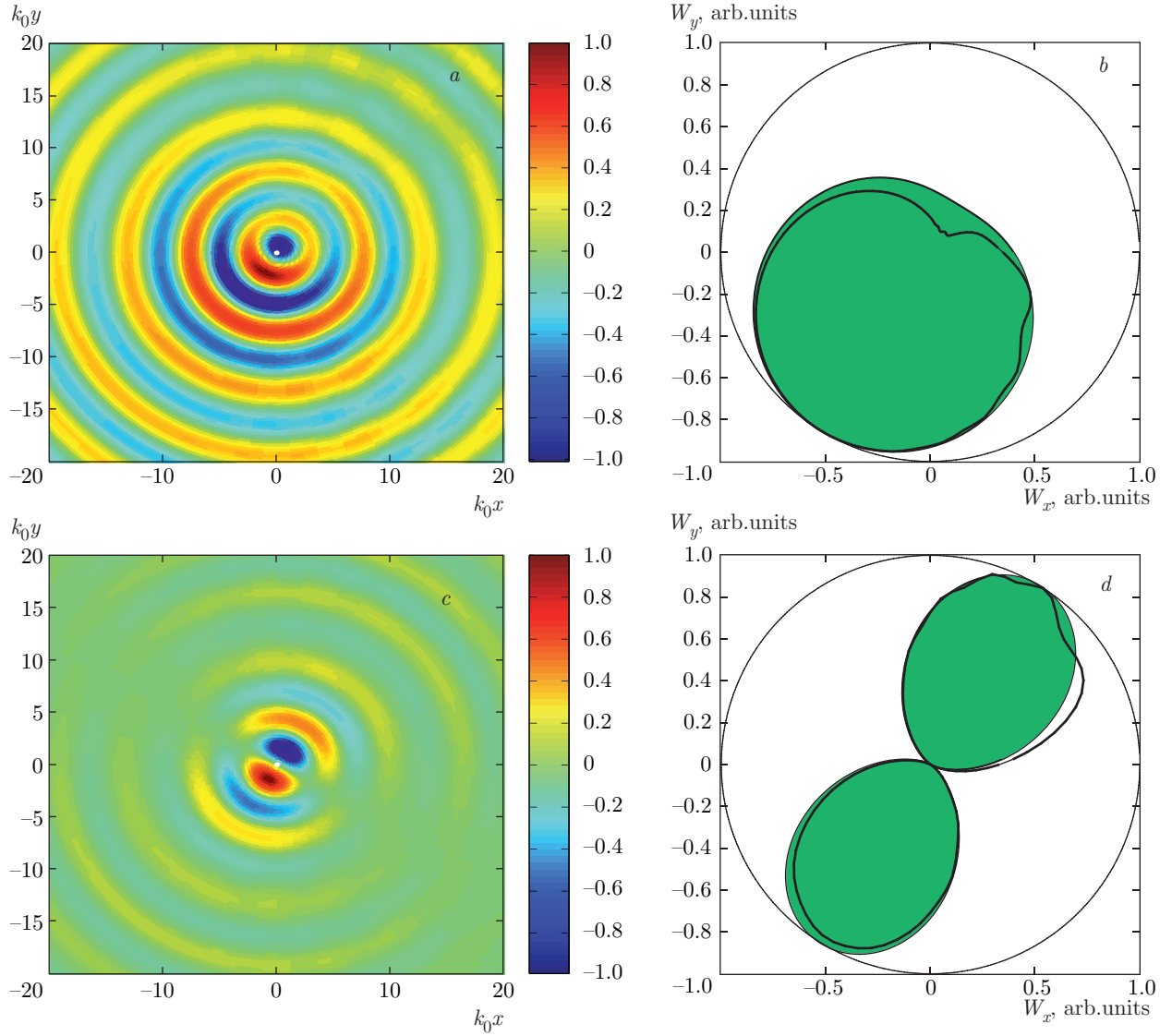
Fig. 9. (a), (c) Spatial structure of the excited SP: the real part of the transverse component of the electric field, $\mathrm{Re}(E_z)$, as a function of (x, y) at the metal–air interface; (b), (d) the corresponding normalized directivity patterns. The case of TM-polarized ligth incident on an elongated elliptical silver nanoparticle is considered for two angles θ. The ratio of ellipsoid semi-axes is $d_\perp/d_\parallel = 0.1$, $n = 0.0205$, $\epsilon_p = \epsilon_m = -7.8191 - 0.7797i$, $\beta = \pi/4$; (a,b) $\theta = \pi/3$, and (c,d) $\theta = 0$; the position of the particle is $k_0 a = 0.1\pi$, and the other parameters are the same as in Fig. 2

4. CONCLUSION

We have studied the so-called photonic spin-dependent optical effects emerging at the SP excitation at an air–metal interface via scattering of light by a dipole nanoparticle located near the interface. It has been shown that the directivity pattern of the excited SP can be managed by means of light polarization, its angle of incidence, and the choice of the nanoparticle position above the interface. These effects demonstrate a promising way to the manipulation of the SP, which can be useful for applications in modern nanoplasmonics. A similar effect of asymmetric SP excitation by linearly polarized light was demonstrated in the example of absorbing nanoparticle with anisotropic polarizability.

REFERENCES

1. P. Kaminov, W. L. Mammel, and H. P. Weber, Appl. Opt. **13**, 396 (1974).

2. M. I. Brongersma and P. G. Kik, *Surface Plasmon Nanophotonics*, Springer-Verlag (2007).

3. S. A. Maier, *Plasmonics*: *Fundamentals and Applications*, Springer-Verlag (2007).

4. I. Cao and M. I. Brongersma, Nat. Photonics **3**, 12 (2009).

5. S. Vedantam, H. Lee, J. Tang, J. Conway, M. Staffaroni, and E. Yablonovitch, Nano Lett. **9**, 3447 (2009).

6. D. K. Gramotnev and S. I. Bozhevolnyi, Nat. Photonics **4**, 83 (2010).

7. M. I. Stockman, Phys. Rev. Lett. **93**, 137404 (2004).

8. A. R. Davoyan, I. V. Shadrivov, A. A. Zharov, D. K. Gramotnev, and Y. S. Kivshar, Phys. Rev. Lett. **105**, 116804 (2010).

9. A. A. Zharov, N. A. Zharova, D. A. Smirnova, and A. A. Zharov, Jr., J. Opt. Soc. Am. B **30**, 626 (2013).

10. A. M. Gobin, M. H. Lee, N. J. Halas et al., Nano Lett. **7**, 1929 (2007).

11. D. J. Bergman and M. I. Stockman, Phys. Rev. Lett. **90**, 027402 (2003).

12. V. M. Menon, L. I. Deych, and A. A. Lisyansky, Nat. Photonics **4**, 345 (2010).

13. D. A. B. Miller, Nat. Photonics **4**, 3 (2010).

14. D. O. O'Connor, P. Ginzburg, F. J. Rodriguez-Fortuno, G. A. Wurtz, and A. V. Zayats, Nat. Commun. **5**, 5327 (2014).

15. K. Y. Bliokh, D. A. Smirnova, and F. Nori, Science **348**, 1448 (2015).

16. J. Petersen, J. Volz, and A. Rauschenbeutel, Science **346**, 67 (2014).

17. B. Le Feber, N. Rotenberg, and L. Kuipers, Nat. Commun. **6**, 6695 (2015).

18. F. J. Rodriguez-Fortuno, G. Marino, P. Ginzburg et al., Science **340**, 328 (2013).

19. C.-F. Li, Phys. Rev. A **80**, 063814 (2009).

20. K. Y. Bliokh and F. Nori, Phys. Rev. A **85**, 061801 (R) (2012).

21. A. Y. Bekshaev, K. Y. Bliokh, and F. Nori, Phys. Rev. X **5**, 011039 (2015).

22. S. V. Li, D. G. Baranov, A. E. Krasnok, and P. A. Belov, Appl. Phys. Lett. **107**, 171101 (2015).

23. N. Rotenberg, M. Spasenovic, T. L. Krijger, B. le Feber, F. J. Garcia de Abajo, and L. Kuipers, Phys. Rev. Lett. **108**, 127402 (2012).

24. N. Rotenberg, T. L. Krijger, B. le Feber, M. Spasenovic, F. Javier Garcia de Abajo, and L. Kuipers, Phys. Rev. B **88**, 241408(R) (2013).

25. J. P. B. Mueller and F. Capasso, Phys. Rev. B **88**, 121410(R) (2013).

26. A. Otto, Z. Physik **216**, 398 (1968).

27. H. Raether, *Surface Plasmons*, Springer-Verlag, Berlin (1988).

28. E. Kretschmann, Z. Physik **241**, 313 (1971).

29. V. M. Agranovich and D. L. Mills, *Surface Polaritons*, North-Holland, Amsterdam (1982).

30. A. D. Boardman, *Electromagnetic Surface Modes*, Wiley, New York (1982).

31. G. I. Stegeman, R. F. Wallis, and A. A. Maradudin, Opt. Lett. **8**, 386 (1983).

32. J. D. Jackson, *Classical Electrodynamics*, Wiley, New York (1962).

33. L. D. Landau and E. M. Livshitz, *Electrodynamics of Continuous Media*, Oxford Pergamon Press (1984).

34. A. A. Zharov and V. V. Kurin, J. Appl. Phys. **102**, 123514 (2007).

33